

Action Potential

John A. White

Boston University

Glossary

activation a term referring to the time- and voltage-dependent growth of a membrane conductance after membrane depolarization

all-or-nothing a term that refers to the property that action potentials, if they occur, have a stereotyped shape that is largely independent of the size and form of the suprathreshold stimulus

current clamp an experimental protocol in which transmembrane current is controlled, usually at a series of constant values, and resulting transmembrane potentials are measured

depolarization making membrane potential less negative

hyperpolarization making membrane potential more negative

inactivation the time- and voltage-dependent decline of the Na^+ conductance, which follows shortly after its activation

membrane potential the voltage difference across the neural membrane

refractory period the period immediately after an action potential, in which it is difficult or impossible to induce a second action potential

space clamp the condition in which membrane potential is the same throughout the spatial extent of the cell

threshold the value of membrane current or membrane potential necessary to induce an action potential

voltage clamp an experimental protocol in which membrane potential is controlled, usually in a stepwise fashion, and resulting transmembrane currents are measured

voltage-gated ion channels transmembrane proteins that open in response to changes in membrane potential, allowing a particular ionic species to cross the membrane

The action potential is the all-or-nothing electrical impulse used to communicate information between neurons and from neurons to muscle fibers. The energy used to generate action potentials comes in the form of electrochemical gradients of ions (in particular, sodium and potassium ions) that are established by ion pumps. The rising phase of action potentials is caused by the auto-catalytic opening of a large number Na^+ -selective ion channels in response to sufficiently large increases in membrane potential. The falling phase of the action potential is caused by two factors which come to dominate the electrical response after a few milliseconds: the tendency of sodium channels to close shortly after they open, and the tendency of potassium channels to open in response to depolarization. The diverse mechanisms underlying electrical excitability in neurons remain a rich field of experimental and theoretical study, with wide-ranging implications for human health.

I. Basic Properties of the Action Potential

The basic properties of the action potential can be studied by first inserting an electrode (constructed from a glass capillary tube with a fine tip and containing artificial intracellular solution) into the cell body or axon of a neuron (Fig. 1a, inset). This electrode will measure the resting value of membrane potential relative to the extracellular space; typical values range from -40 to -90 mV. Passing positive electrical current into the cell *depolarizes* it (i.e., makes membrane potential less negative). In response to small depolarizing stimuli, the neuron's response is small as well (Fig. 1a, bottom panel). In response to larger stimuli, above a threshold value, the response is fundamentally different: membrane potential quickly rises to a value well above 0 mV, then falls over the course of 1-5 ms to its resting value (Fig. 1a, middle panel). Often, the falling phase of the action potential undershoots resting potential temporarily. The action potential is said to be *all-or-nothing* because it occurs only for sufficiently large depolarizing stimuli, and because its form is largely independent of the stimulus for supra-threshold stimuli. In some neurons, a single action potential can be induced by the *offset* of a hyperpolarizing stimulus (Fig. 1b). This phenomenon is called *anode-break excitation* or *rebound spiking*.

The value of threshold depends on the duration of the stimulus (Fig. 1c); brief stimuli are required to be larger to evoke an action potential. Threshold also depends on more subtle features of the stimulus, such as its speed of onset. For a short time after an action potential has occurred, it is impossible to evoke a second one (Fig. 1d). This period is referred to as the *absolute refractory period (ARP)*. After the absolute refractory period comes the *relative refractory period (RRP)*, in which an action potential can be evoked, but only by a larger

stimulus than was required to evoke the first action potential. Stimulation by an ongoing supra-threshold stimulus leads to repetitive firing at a rate that is constant once any transients have settled out (Fig. 2a). The rate of repetitive firing increases with increasing depolarization (Fig. 2b), eventually approaching the limit imposed by the absolute refractory period.

Once initiated, the action potential propagates down the axon at an approximately constant velocity. The leading edge of the action potential depolarizes adjacent unexcited portions of the axon, eventually bringing them to threshold. In the wake of the action potential, the membrane is refractory, preventing re-excitation of previously active portions of the cell. In unmyelinated axons, the action potential travels smoothly, with constant shape and at constant velocity. In myelinated axons, conduction is saltatory: the action potential “jumps” nearly instantaneously from one node of Ranvier to the next, greatly increasing the speed of propagation.

II. Classical Descriptions of the Action Potential

A. *Electrochemical Potentials and Voltage-Dependent Membrane Conductances in Excitable Cells*

Changes in electrical potential in excitable cells are driven by movement of ions through ion-specific membrane conductances. For a perfectly specific conductance G , the current that flows across the membrane $I = G \times (V_m - V_n)$, where V_m is the electrical potential across the membrane and V_n is the *equilibrium potential* for the ion, given by the Nernst equation:

$$V_n = \frac{RT}{z_n F} \ln \left(\frac{[X_n]^o}{[X_n]^i} \right)$$

where $R = 8.314 \text{ J}/(\text{mol K})$ is the gas constant, T is absolute temperature, z_n is the valence of ion n , $F = 9.648 \times 10^4 \text{ C}/\text{mol}$ is Faraday's constant, $[X_n]^o$ is the outer concentration of ion n , and $[X_n]^i$ is the inner concentration of ion n . Intuitively, the equilibrium potential is the value of membrane potential at which ionic fluxes due to concentration gradients and voltage gradients cancel one another, leading to zero net flux of the ion. Note that ionic current, as defined, is positive for outward flux of a positive ion. For neurons, $[\text{Na}^+]^o > [\text{Na}^+]^i$; consequently V_{Na} typically ranges from 40 to 50 mV and $I_{\text{Na}} < 0$. In contrast, $[\text{K}^+]^i > [\text{K}^+]^o$, V_{K} ranges from -70 to -100 mV, and $I_{\text{K}} > 0$. The fact that resting membrane potential is far from V_{Na} , and close but typically not equal to V_{K} , implies that these ions are out of equilibrium, and thus that there is a constant trickle of each, even at rest. This flux is opposed by energy-expending ionic pumps, most notably the Na^+/K^+ ATPase, which serve to maintain Na^+ and K^+ concentration gradients and, consequently, equilibrium potentials.

Among the first quantitative clues regarding the mechanisms underlying the action potential came from ionic substitution experiments demonstrating that Na^+ and K^+ are the primary ions responsible for the phenomenon. Other early experiments demonstrated that membrane conductance, but not membrane capacitance, changes during the course of the action potential. Together, these results suggested the (correct) hypothesis that fluxes of Na^+ and K^+ , driven by changes in ion-specific conductances, are responsible for the action potential. It is important to note that changes in membrane potential are not induced by changes in intracellular concentrations of Na^+ and K^+ : ionic fluxes during individual action potentials are small enough that concentrations remain essentially unperturbed. Instead, ionic fluxes alter V_m by changing the *distribution* of charge very near the membrane.

B. The Hodgkin-Huxley Model of the Space-Clamped Action Potential

Researchers in the middle of the 20th century hypothesized that the Na⁺ and K⁺ conductances underlying the action potential are “gated” (i.e., turned on and off) by changes in membrane potential. To test this hypothesis, they devised methods to measure ionic fluxes while controlling membrane potential V_m at a fixed value throughout the length of the axon. The process of controlling V_m , called *voltage clamping*, simplifies the behavior of the hypothesized voltage-dependent “gates”. The process of making V_m the same throughout the axon, called *space clamping*, prevents complex spatial spread of excitation. Under these conditions, Na⁺ and K⁺ fluxes can be isolated either by manipulation of ionic concentrations (and thus equilibrium potentials), or by using specific blockers of particular conductances. (Tetrodotoxin, or TTX, is the classic blocker of Na⁺ conductances; tetraethyl ammonium, or TEA, blocks many K⁺ conductances.) Isolated Na⁺ and K⁺ fluxes from simulations are shown in Fig. 3 for a number of values of membrane potential. As hypothesized, these fluxes are voltage-dependent. Na⁺ and K⁺ fluxes differ in several important regards. First, they are opposite in sign for most values of membrane potential: the Na⁺ flux depolarizes the neuron, while the K⁺ flux hyperpolarizes the cell. Second, the Na⁺ flux turns on (“activates”) much more quickly than the K⁺ flux. Third, the Na⁺ flux turns itself off (“inactivates”) after a brief period of depolarization. In contrast, the K⁺ conductance remains activated in response to a prolonged depolarizing stimulus.

A watershed event in the history of neuroscience was the development by Hodgkin and Huxley of a relatively simple mathematical model, derived from voltage-clamp studies of the giant axon of the squid, that accounts for the generation and propagation of the action potential. The Hodgkin-Huxley model describes the membrane as an electrical circuit (Fig. 4a) that includes

descriptions of membrane capacitance C_m ; voltage-gated, Na^+ - and K^+ -selective conductances (G_{Na} and G_{K} , respectively), each in series with a battery representing the appropriate equilibrium potential; and a constant “leak” conductance that passes more than one ion. Mathematically, the Hodgkin-Huxley model includes 4 differential equations, which describe how the derivatives of membrane potential and 3 “gating variables” (variables that range between zero and one and determine the values of voltage-gated conductances) behave. Two time- and voltage-dependent gating variables determine the size of the Na^+ conductance: the m -gate captures the rapid *activation* of the Na^+ conductance after a step depolarization, whereas the h -gate describes the somewhat slower *inactivation* process by which the Na^+ conductance turns itself off. One gating variable, the n -gate, describes voltage-dependent activation of the K^+ conductance G_{K} . An additional conductance (the leak conductance G_{L}) is voltage-*independent* and small. In mathematical terms, the Hodgkin-Huxley equations are written as follows, with symbols defined in Table I.

$$C_m \frac{dV_m}{dt} = -[G_{\text{Na}}(V_m - V_{\text{Na}}) + G_{\text{K}}(V_m - V_{\text{K}}) + G_{\text{L}}(V_m - V_{\text{L}})] + I_{\text{app}}$$

$$G_{\text{Na}} = \bar{G}_{\text{Na}} m^3 h \quad G_{\text{K}} = \bar{G}_{\text{K}} n^4$$

$$\frac{dm}{dt} = \frac{m_{\infty}(V_m) - m}{\tau_m(V_m)} \quad \frac{dh}{dt} = \frac{h_{\infty}(V_m) - h}{\tau_h(V_m)} \quad \frac{dn}{dt} = \frac{n_{\infty}(V_m) - n}{\tau_n(V_m)}$$

In response to a step change from an initial value of membrane potential (often referred to as the holding potential, V_{hold}) to the clamp potential, V_{clamp} , each of the Hodgkin-Huxley gating variables (m , h , and n) changes from an initial value to a steady-state value with an exponential time course (Figs. 4b-c). The steady-state values (m_{∞} , h_{∞} , and n_{∞}) and exponential time constants (τ_m , τ_h , and τ_n) are determined solely by the current value of V_m , which equals V_{clamp} for voltage-clamp experiments (Figs. 4e-f). The initial values of the gating variables are determined by the

holding potential. G_{Na} is proportional to $m^3 \times h$; G_K is proportional to n^4 (Figs. 4b-d). The powers to which the gating variables m and n are raised were used by Hodgkin and Huxley to induce small delays in activation of the conductance, in order to better match experimental data.

C. The Hodgkin-Huxley Model Accounts for the Basic Properties of the Action Potential

Although the Hodgkin-Huxley model is incorrect in some details (see Section IIIA), it can account for many of the basic properties of the neuronal action potential. For example, two properties of the m -gate account for the phenomenon of the all-or-nothing action potential with a distinct threshold in response to a particular type of stimulus. First, because the m -gate activates (opens) with depolarization, and its activation leads to further depolarization, this gate is prone to auto-catalytic “positive feedback” that can magnify a small depolarization into a full-blown action potential. The current threshold for firing an action potential is the amount of current required to engage this cycle of positive feedback (see Section IIID for a discussion of the threshold value of membrane potential). In contrast with the m -gate, the h - and n - gates react to oppose depolarization (h because it gets smaller with depolarization, n because its activation increases the size of an outward K^+ current). The second crucial feature of the m -gate is it is much faster than the h - and n -gates (Fig. 4e). The speed of the m -gate means that the rapid rising phase of the action potential can occur before the stabilizing influences of the h - and n -gates can engage to bring V_m back down near resting potential. The speed of inactivation of h (i.e., its decrease with depolarization) and activation of n determine the width of the action potential. Traces of each of the gating variables during the course of a depolarization-induced action potential are shown in Fig. 5a. The phenomena of absolute and relative refractory periods can be

accounted for by tracking gating variables as well. The absolute refractory period (ARP) is associated with elevated values of n and, most importantly, greatly reduced values of h after a spike (Fig. 5a). These factors make it impossible for a second spike to be elicited soon after the first. The relative refractory period (RRP) lasts as long as it takes for the h - and n -gates to return to their baseline values – about 15 ms in squid giant axon.

At resting potential, the voltage-gated Na^+ conductance is partially inactivated, in that the h -gate is partly closed and the n -gate is partly open (Figs. 4-5; as we shall see, having gates partially open implies that the open probabilities of ion channels are less than one) Hyperpolarizing the neuron below resting potential increases the value of h , in a process called *deinactivation*, and decreases the value of n , in a process called *deactivation*. Deinactivation of the Na^+ conductance and deactivation of the K^+ conductance can leave the neuron more excitable after hyperpolarization, and thus account for anode-break excitation (Fig. 5b), also known as rebound spiking. Neurons typically fire only one rebound spike because, after that spike, the Na^+ and K^+ conductances return to their baseline states and the cell has returned to its resting level of excitability.

The first great success of the Hodgkin-Huxley model was that this relatively simple model, derived from voltage-clamp experiments, accounted successfully for many aspects of the action potential in the current-clamped and space-clamped axon. Even more impressive, and strikingly demonstrative of the level of understanding this model represents, was its ability to account accurately for the shape and velocity of the propagating action potential. The quantitative arguments involved are complex and will not be covered here, but Fig. 6 shows qualitatively how action potentials propagate in unmyelinated axons. Membrane potential reaches its peak

value near the position of maximal Na^+ flux. Adjacent, unexcited membrane (to the right in the figure) is depolarized by positive current from the site of Na^+ flux. Eventually, this depolarization is large enough that the membrane at the leading edge is excited as well. The membrane in the wake of the action potential is refractory (i.e., dominated by small G_{Na} and large G_{K} , and thus unable to spike), and thus unlikely to be re-excited. Elaborations of this model can account for saltatory conduction in myelinated axons.

III. Modern Topics Related to the Action Potential

A. *Voltage-Gated Ion Channels Underlie Voltage-Dependent Membrane Conductances*

In the last two decades, improvements in recording methodologies, pioneered by the group of Sakmann and Neher, as well as an explosion of knowledge in the field molecular biology, have demonstrated directly that membrane-protein assemblies called *ion channels* underlie voltage-gated conductances in neurons and other excitable cells. The main (α) subunit of voltage-gated Na^+ channels (Fig. 7a) is a membrane protein that is roughly 2000 amino acids in length and has a molecular weight $> 200,000$. This protein includes 4 domains, each of which consists of 6 putative transmembrane segments. A smaller β -subunit is not necessary to form the channel, but is crucial for regulating aspects of channel function like the speed of inactivation. The main subunit of the K^+ channel has a very similar structure, except that the each protein codes for only one domain. Thus, four α -subunits are necessary to form a K^+ channel.

Recordings from single channels (Fig. 7b) typically reveal two conductance states: ‘open’ and ‘closed’. Switching between open and closed states appears random, but the probability that the

channel is in the open state varies with membrane potential. These probabilities roughly correspond to the values of gating variables in the Hodgkin-Huxley formulation. Sums of repeated recordings from an individual ion channel show behavior that is very similar to the macroscopic behavior of the channel population (Fig. 7b). Sophisticated analyses of single-channel recordings yield probabilistic models that can account for both microscopic and macroscopic behavior. These models are similar in structure to Hodgkin-Huxley-type models, but different in some details. For example, careful analysis of recordings from single Na⁺ channels shows that their inactivation state is not controlled by an activation-independent process like the *h*-gate, but rather that Na⁺ channels must activate *before* they can inactivate.

Experiments with channels that have been subjected to site-directed mutations have revealed close connections between particular loci on the protein and specific aspects of channel behavior. Among the properties that have been tied to specific loci on the α -subunit are those of pore formation, ionic selectivity, voltage-dependence, inactivation, and blockage by specific toxins (Fig. 7a).

B. Diversity of Mechanisms Contributing to Neuronal Excitability

In the half-century since the development of the Hodgkin-Huxley model, researchers have discovered a large number of ion-channel-based mechanisms for generating and controlling electrical activity in neurons. Most often, these mechanisms rely on Na⁺, Ca²⁺, and K⁺ channels. Sodium channels are relatively consistent in their properties from case to case, but do show some variety. In particular, some Na⁺ channels do not exhibit fast inactivation; as of yet, it is not clear whether these non-inactivating Na⁺ channels are a separate population from the typical, fast-inactivating Na⁺ channels, or a subset of the fast-inactivating Na⁺ channels that have slipped into

a different “mode” of gating. Calcium and potassium channels show more diversity than Na^+ channels. In particular, different classes of Ca^{2+} and K^+ channels show widely diverse properties with regard to the presence and speed of inactivation, pharmacological properties, and voltage ranges of activation. Some K^+ channels are sensitive to both membrane potential and the local intracellular concentration of Ca^{2+} , giving rise to interesting interactions between these two systems.

C. Modulation of Voltage-Gated Ion Channels

The properties of voltage-gated ion channels are not static. A large number of neuromodulators have been shown to alter ion-channel function and the properties of action potentials by phosphorylating or dephosphorylating one or more sites on the channel protein. A host of neuronal firing properties, including spike width, average firing rate, and refractory period, are subject to metabolic control.

Ion-channel expression profiles and neuromodulatory states can have profound consequences for neuronal function. A striking example of this point comes from thalamic relay neurons (Fig. 8). Depending on the level of depolarization or neuromodulatory state, these cells have two distinct firing “modes.” When relay neurons are hyperpolarized, they exhibit rhythmic bursting (Fig. 8a). The long inter-burst interval is determined by interaction of the low-threshold Ca^{2+} current and slowly activating, inwardly rectifying cation current. Superimposed on each slow Ca^{2+} spike are a number of fast action potentials, mediated by Na^+ and K^+ channels. When relay neurons are depolarized, either by electrical current or any of a number of neuromodulators, the low-threshold Ca^{2+} channels and inwardly rectifying cation channels are unimportant and the neurons fire in a tonic pattern much more reminiscent of the Hodgkin-Huxley model (Fig. 8b).

D. Mathematical Analyses of Neuronal Excitability

Although much about neuronal excitability can be learned by simply tracking changes in gating variables of Hodgkin-Huxley-style model, computational neuroscientists and applied mathematicians have used mathematically-based techniques to gain more general (and thus deeper) insights. Mathematical approaches, based on the techniques of *nonlinear dynamics*, have been successful in identifying the particular features that determine a host of important features of neuronal excitability, including threshold, the relationship between sustained firing rates and applied current, and particular patterns of bursting.

Figure 9 shows how nonlinear dynamics can be applied to understand neuronal threshold. Panels a-b show results from simulations of the Hodgkin-Huxley equations with zero applied current, but two different initial conditions in membrane potential. As the panels demonstrate, excitable cells can be exquisitely sensitive to initial conditions. Examining the time derivative of membrane potential $\dot{V}_m(t)$ shortly after the perturbation in initial conditions gives insight into this phenomenon. Figure 9c shows results from hundreds of simulations conducted over a large range of initial values V_0 . $\dot{V}_m(t)$, evaluated at $t = 0.5$ ms, is plotted vs. V_0 (solid line; the value $t = 0.5$ ms was chosen because this is long enough for the m -gate to react significantly to the perturbation away from resting potential, but short enough that the h - or n -gates remain relatively near their resting values). Also plotted are the contributions to $\dot{V}_m(0.5)$ from Na^+ conductance (dashed line), as well as K^+ and leak conductances (dotted line). These contributions can be obtained easily from the Hodgkin-Huxley equation describing $\dot{V}_m(t)$. The effect of the Na^+ conductance is to elevate $\dot{V}_m(t)$; the effect of the K^+ conductance is to reduce $\dot{V}_m(t)$.

Figure 9d shows a magnified view of $\dot{V}_m(0.5)$ in the region near spike threshold. The plot shows two zero-crossings, at $V_0 = -65$ and -59 mV. These zero-crossings, often called *fixed points*, are especially important because, where $\dot{V}_m(t) = 0$, membrane potential V_m is by definition not changing, meaning that V_m has the potential to remain fixed at that point indefinitely (for a system with constant parameters). The *slope* of the curve at each zero-crossing tells us much about the *stability* of that fixed point in response to small fluctuations (e.g., due to noise). For example, consider the special case of no perturbation. In this case, V_0 equals resting potential (-65 mV), which we expect to be a fixed point. For V_m slightly less than -65 mV, $\dot{V}_m(0.5) > 0$, implying that V_m will return to its resting value. For V_m slightly greater than -65 mV, $\dot{V}_m(0.5) < 0$, implying again that V_m will return to -65 mV. The value $V_m = -65$ mV is said to be a *stable fixed point*, because after small perturbations above or below that value, V_m will return.

Next, consider the fixed point at $V_0 = -59$ mV. In this case, $\dot{V}_m(0.5) < 0$ for $V_m < V_0$ and $\dot{V}_m(0.5) > 0$ for $V_m > V_0$. This result implies that this fixed point is *unstable*: after small perturbations above or below V_0 , V_m will move away from the fixed point. The implication of this fact is that the point $V_0 = -59$ mV serves as a *threshold*. For $V_0 < -59$ mV, the model returns to resting potential (e.g., Fig. 9a); for $V_0 > -59$ mV, V_m rapidly increases as the action potential begins (Fig. 9b; in these cases, $\dot{V}_m(t)$ continues to evolve, eventually bringing the cell to rest). For these simulations, the fixed point at $V_0 = -59$ mV corresponds exactly with the threshold for generation of an action potential (vertical dashed line in Fig. 9d).

E. Back-Propagation of the Action Potential

In the traditional view, information flow in the mammalian neuron is in one direction only: the dendrite receives input from the presynaptic population; the soma integrates this information; the decision regarding whether or not to fire an action potential is made at or near the axon hillock; and the action potential is propagated to other neurons by the axon. This view has been amended in recent years, as scientists have developed techniques for recording simultaneously from multiple locations within the neuron (e.g., the soma and a primary dendrite). In pyramidal neurons of layer V of neocortex, for example, suprathreshold synaptic input to the apical dendrites leads to initiation of an action potential near the soma. This action potential can then travel back from the soma toward the distal end of the apical dendrite. The reliability of back-propagation depends on spiking history in a complex manner. Given the crucial role of dendritic depolarization for synaptic plasticity, back-propagating action potentials may be important for experience-dependent alterations of neuronal circuitry in learning and memory.

F. Diseases Related to Mutations in Ion Channels

Given the central role that electrical excitability plays in nervous system function, it is not surprising that mutations of voltage-gated ion channels alter neuronal function. Although work in this area is just beginning, a host of maladies have been associated with non-lethal mutations of neuronal voltage-gated channels. For example:

- *Generalized epilepsy with febrile seizures*, so-named because patients start with fever-induced seizures that develop later in life into seizures without a clear trigger, is associated in some cases with a rare mutation of the β_1 subunit of the Na^+ channel. This mutation may

promote epilepsy by slowing the inactivation process in neuronal Na⁺ channels, leaving the brain hyper-excitabile.

- *Benign familial neonatal epilepsy* is associated with mutations that lead to reduced expression of slow, voltage-gated K⁺ channels of the KCNQ family, thereby leaving some neurons hyper-excitabile.
- Some forms of *episodic ataxia*, a condition of triggered events of imbalance and uncoordinated movements, has been tied to a number of missense mutations of the K_v1.1 channel, which gives rise to an inactivating K⁺ conductance. Ataxia-associated mutations of K_v1.1 have been shown to lead to pathologically rapid deactivation, enhanced inactivation, and increases in the threshold of activation. This disparate changes all have the effect of broadening the neuronal action potential, but it is not known how the broadened spike may lead to ataxia.

Bibliography

Aidley, D. J. and Stanfield, P. R. (1996) *Ion Channels: Molecules in Action*. Cambridge University Press, Cambridge, UK.

Ashcroft, F. M. (2000) *Ion Channels and Disease*. Academic Press, San Diego, CA.

Hille, B. (1992) *Ionic Channels of Excitable Membranes*, 2nd edition. Sinauer Associates, Sunderland, MA, USA.

Johnston, D. and Wu, S. M.-S. (1995) *Foundations of Cellular Neurophysiology*. MIT Press, Cambridge, MA, USA.

Koch, C. (1999) *Biophysics of Computation*. Oxford University Press, New York, USA.

Koch, C. and Segev, I. (Eds.). (1998) *Methods in Neuronal Modeling*, 2nd edition. MIT Press, Cambridge, MA, USA.

Nicholls, J. G., Martin, A. R., and Wallace, B. G. (1992) *From Neuron to Brain*, 2nd edition. Sinauer Associates, Sunderland, MA, USA.

Sakmann, B. and Neher, E. (Eds.). (1995) *Single-Channel Recording*, 2nd edition. Plenum Press, New York.

Stuart, G., Spruston, N., Sakmann, B., and Häusser, M. Action potential initiation and backpropagation in neurons of the mammalian CNS. *Trends in Neurosciences* 20: 125-131.

Weiss, T. F. (1996) *Cellular Biophysics*. MIT Press, Cambridge, MA, USA.

White, J. A., Rubinstein, J. T., and Kay, A. R. (2000) Channel noise in neurons. *Trends in Neurosciences* 23: 131-137.

Figure Legends

Figure 1. Basic properties of the action potential. *a.* Traces show responses of a simulated space-clamped squid axon ($T = 6.3^{\circ}\text{C}$) to intracellularly injected current pulses of duration 0.5 ms (top trace). The simulated recording configuration is shown in the inset. Sufficiently large inputs evoke all-or-nothing action potentials (middle trace). The response is minimal to subthreshold stimuli (bottom trace). The inset shows the basic recording configuration. *b.* A simulation demonstrating anode-break excitation in response to the offset of a hyperpolarizing current pulse (duration = 10 ms). *c.* Current threshold (the minimal amplitude of a current step necessary to evoke an action potential), plotted vs. stimulus duration. *d.* Simulation results demonstrating refractoriness. Two current pulses (duration = 0.5 ms each) were delivered to the model, with interstimulus interval (ISI) varied systematically. The first pulse had magnitude twice the threshold for evoking an action potential. The y-axis shows the magnitude of the second pulse necessary to evoke a spike. For $\text{ISI} < 15$ ms, threshold is above its normal value (dashed line). During the relative refractory period (RRP), threshold is elevated; during the absolute refractory period (ARP), it is not possible to evoke a second action potential.

Figure 2. Spike rate depends on the magnitude of applied current. *a.* Simulated traces of space-clamped squid giant axon ($T = 6.3^{\circ}\text{C}$) to constant applied current. *b.* Firing rate grows with increasing applied current. Note that the minimal firing rate is well above zero spikes/s.

Figure 3. Simulated responses to voltage-clamp stimuli. Simulated Na^+ (*a*) and K^+ (*b*) in response to voltage-clamp steps from a holding potential of -90 mV to clamp potentials of -80 (solid lines), -40 (dashed), 0 (dotted), and $+40$ (dashed-and-dotted) mV. The Na^+ flux is inward

(negative) and is characterized by rapid activation and somewhat slower inactivation. The K^+ flux is outward (positive) and activates significantly more slowly than the Na^+ flux.

Figure 4. The Hodgkin-Huxley model of voltage-gated Na^+ and K^+ conductances. *a*:

Electrical circuit representation of the Hodgkin-Huxley model of squid giant axon under space-clamped conditions. ***b-d***: Responses of the Hodgkin-Huxley gating variables to a voltage-clamp step from $V_{hold} = -90$ mV to $V_{clamp} = 0$ mV. The *m*- and *h*-gates determine the value of $G_{Na} \propto m^3 h$. The *n*-gate determines the value of $G_K \propto n^4$. ***e***: Steady-state values of *m*, *h*, and *n* for the entire physiologically relevant range of membrane potential V_m . ***f***: Time constants describing how quickly the gating variables *m*, *h*, and *n* reach their steady-state values, plotted vs. V_m . Note the log scale on the y-axis.

Figure 5. The Hodgkin-Huxley model accounts for axonal excitability. *a*:

From top to bottom, applied current I_{app} , membrane potential V_m , and each of the gating variables is plotted vs. time. Curves were derived from the Hodgkin-Huxley model at 6°C. The rapid activation of the *m*-gate underlies the action potential in response to this brief current pulse. The slower inactivation of the *h*-gate and activation of the *n*-gate repolarize the membrane a few milliseconds later. The duration of the absolute and relative refractory periods (ARP and RRP, respectively) are controlled by the duration of *h*-gate inactivation and *n*-gate activation. ***b***: After a hyperpolarizing input, the Hodgkin-Huxley model (6°C, with enhanced density of the Na^+ conductance) can produce a rebound spike (also known as anode break excitation). Data are plotted in the same order as in *a*. Deactivation of the *n*-gate and deinactivation of the *h*-gate underlie this phenomenon.

Figure 6. Propagation of the action potential in an unmyelinated axon. *Top:* Schematic of the unmyelinated axon, showing the sequence of events as an action potential propagates from left to right. The point of maximal Na^+ flux characterizes the locus where V_m is greatest. Positive charge from this point spreads to the right, gradually depolarizing the membrane on the leading edge of the action potential until threshold is reached. At the trailing edge of the action potential, to the left, the membrane is refractory. *Bottom:* “Snapshot” of V_m plotted vs. axial distance for the propagating action potential, with an assumed conduction velocity of 20 m/s. Note that the form of the action potential is reversed when plotted vs. distance rather than time.

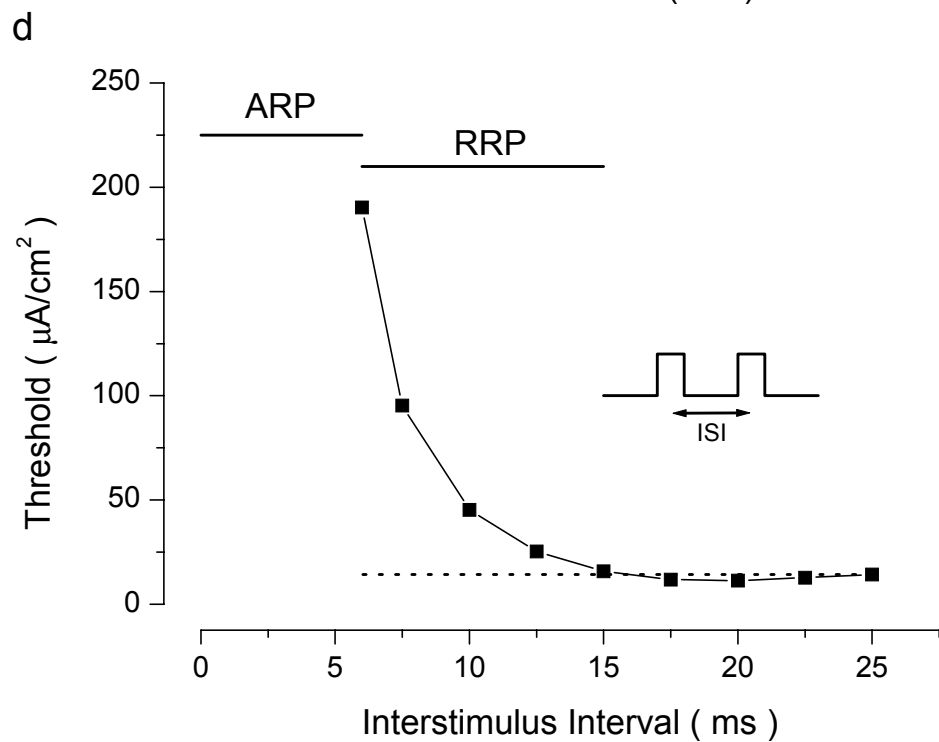
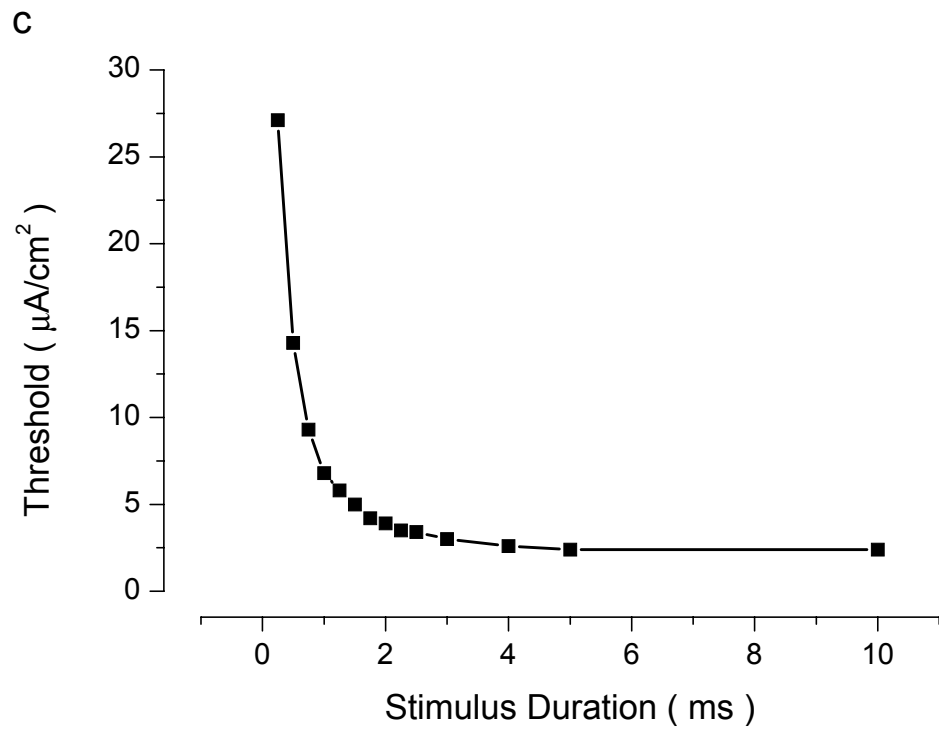
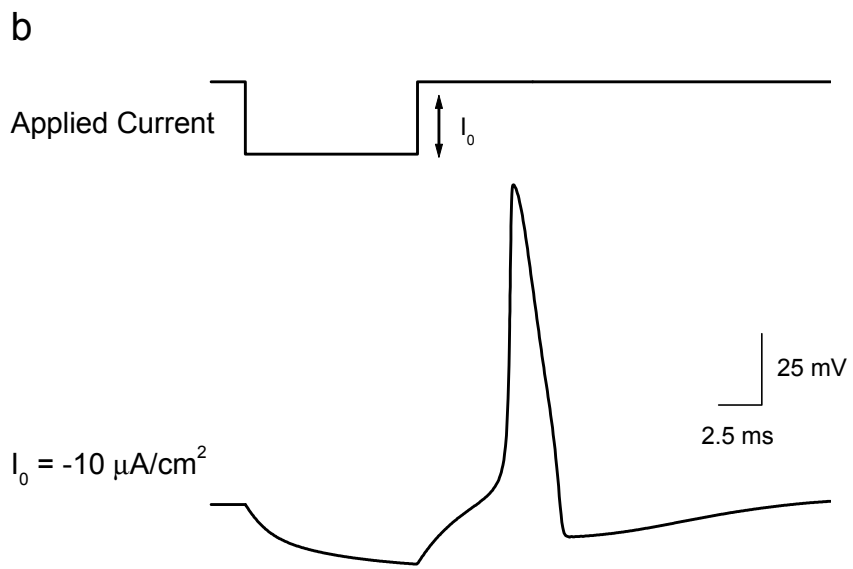
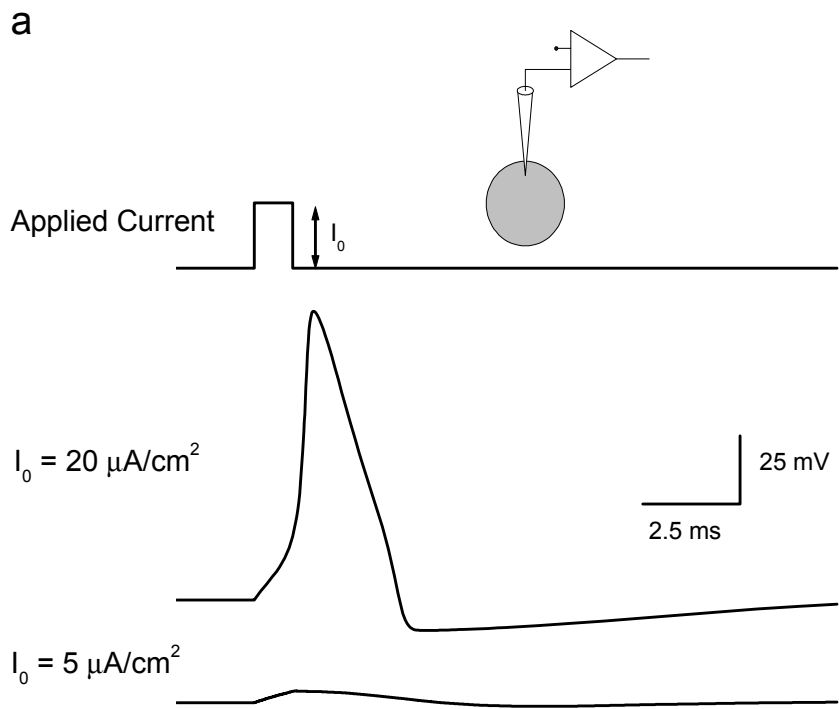
Figure 7. Na^+ channels underlie the voltage-gated Na^+ conductance. *a.* Putative structure of the α - and β -subunits of the rat brain Na^+ channel (IIA). Roman numerals indicate the domains of the α -subunit, each of which includes 6 putative transmembrane segments. Indicated residues are implicated in binding the channel blocker tetrodotoxin (E387), and in forming the inactivation gate (IFM 1488-1490). Adapted from Ashcroft, F. M. (2000) *Ion Channels and Disease*. Academic Press, San Diego, CA. *b.* The 10 middle traces show simulated single-channel recordings from a Na^+ channel under voltage clamp. The top trace shows the voltage-clamp command. The bottom trace shows the sum of 625 single-channel records.

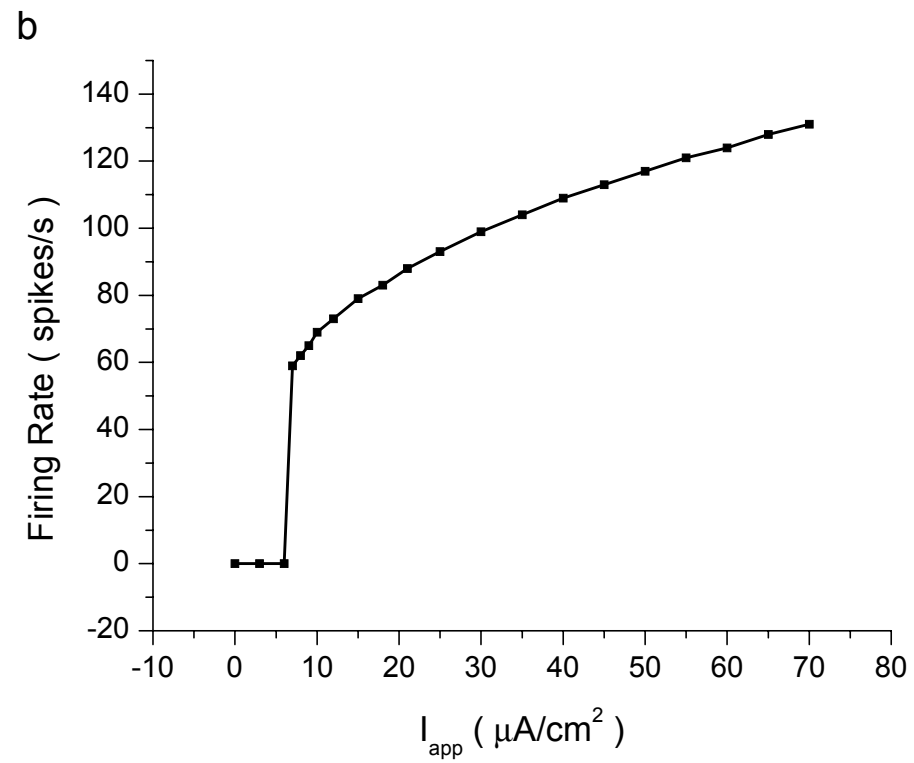
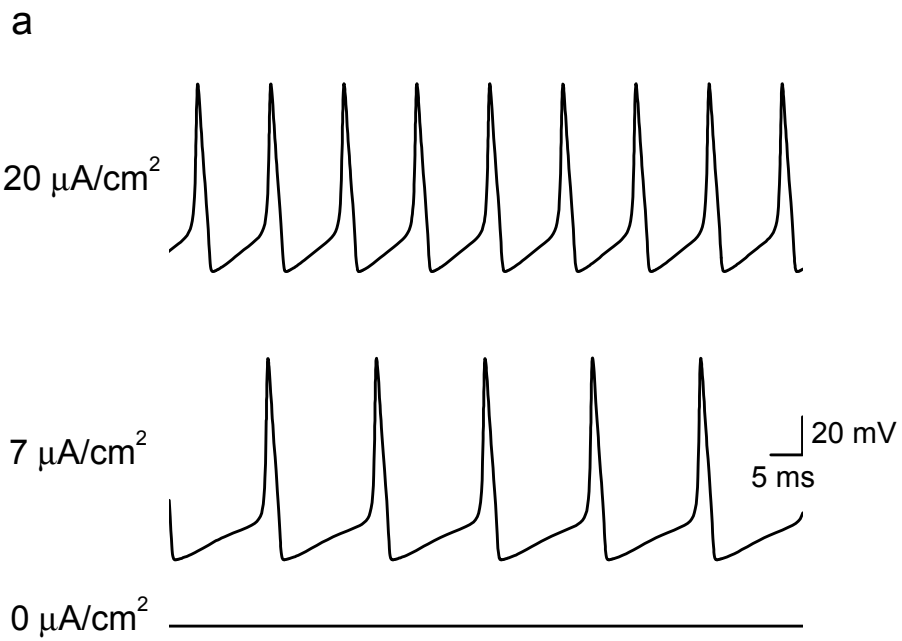
Figure 8. Thalamic relay neurons show two distinct firing modes. Shown are simulated responses of a thalamic relay neuron [McCormick, D. A. and Huguenard, J. R. (1992) A model of the electrophysiological properties of thalamocortical relay neurons. *J. Neurophysiol.* 68: 1384-1400]. *a.* Under hyperpolarized conditions, relay neurons fire in an oscillatory manner. Slow oscillations are generated by interactions of the transient Ca^{2+} current I_t and the slow, hyperpolarization-activated cation current I_h . Fast action potentials, mediated by Na^+ and K^+ ,

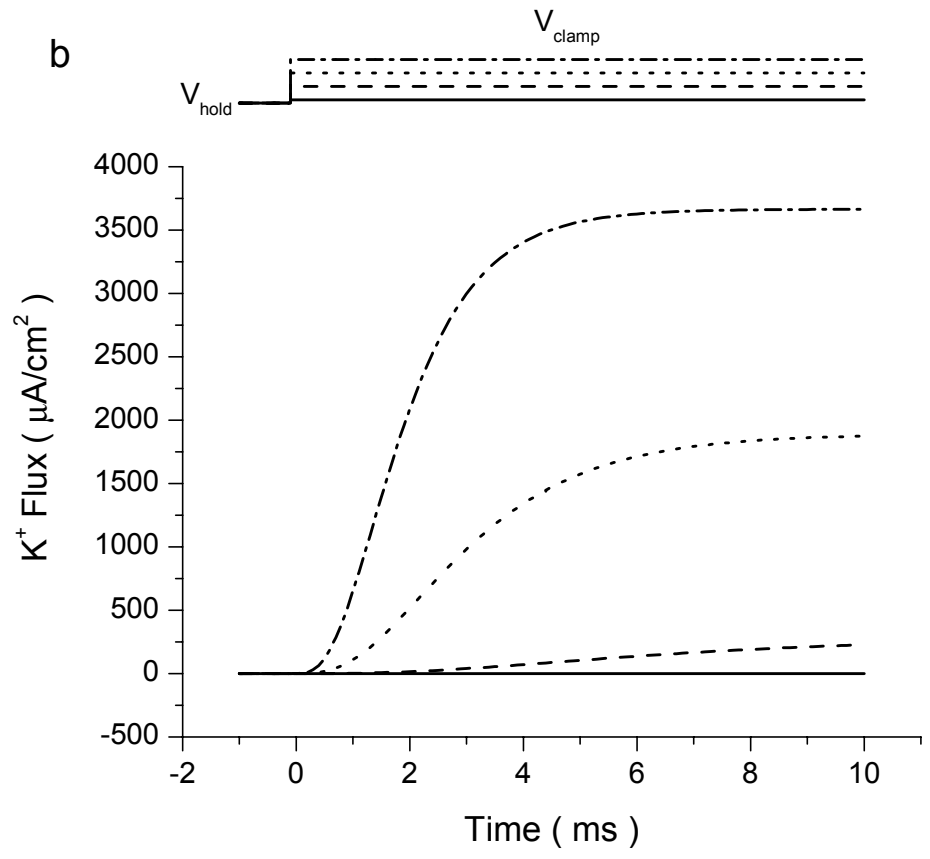
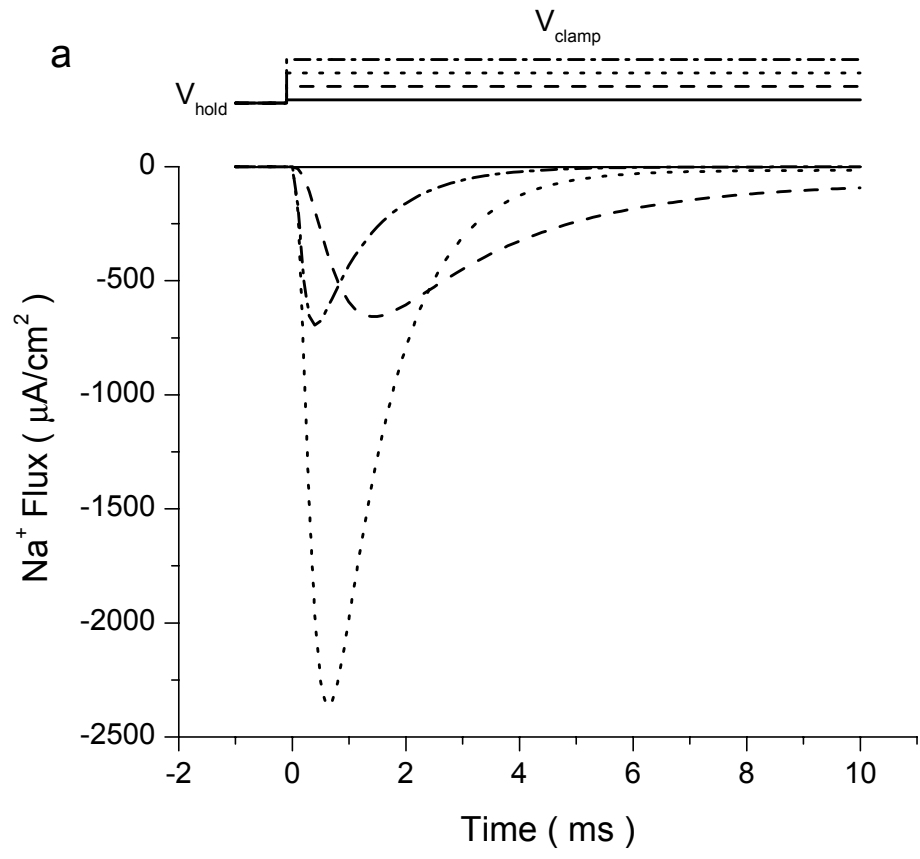
occur at the peaks of the Ca^{2+} spikes. **b.** Depolarization by any of a number of means (e.g., current injection or neuromodulation) puts the neuron in a “tonic firing” mode. In this mode, I_t is inactivated and I_h is deactivated. Consequently, the cell’s behavior is dominated by the Na^+ and K^+ currents exclusively.

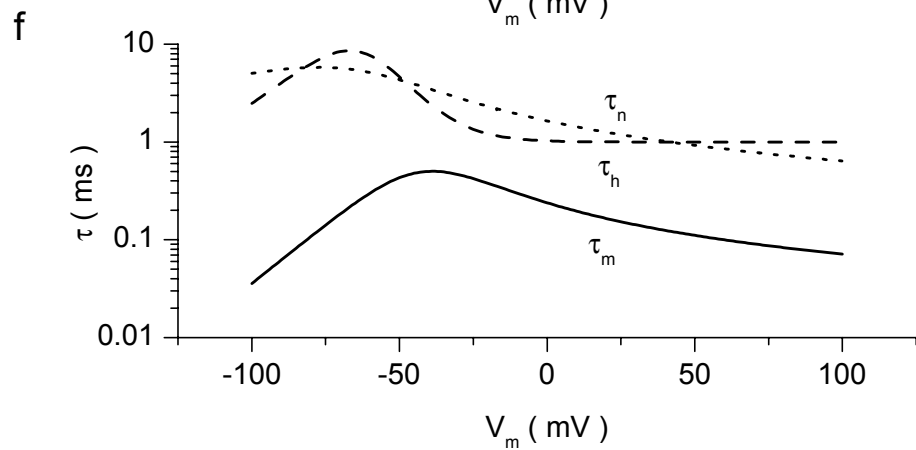
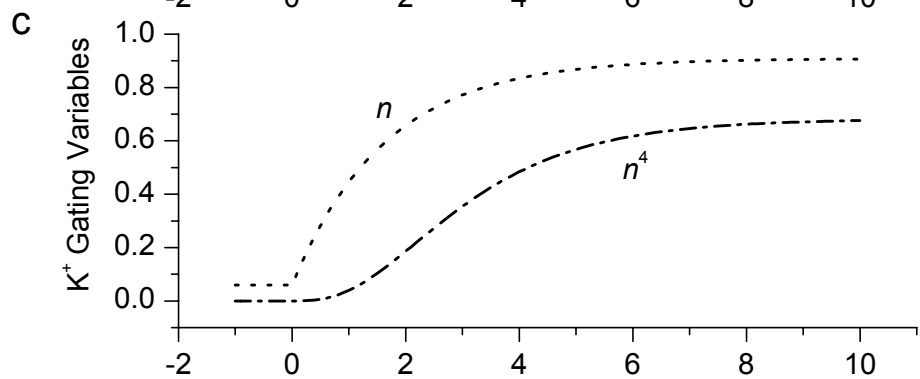
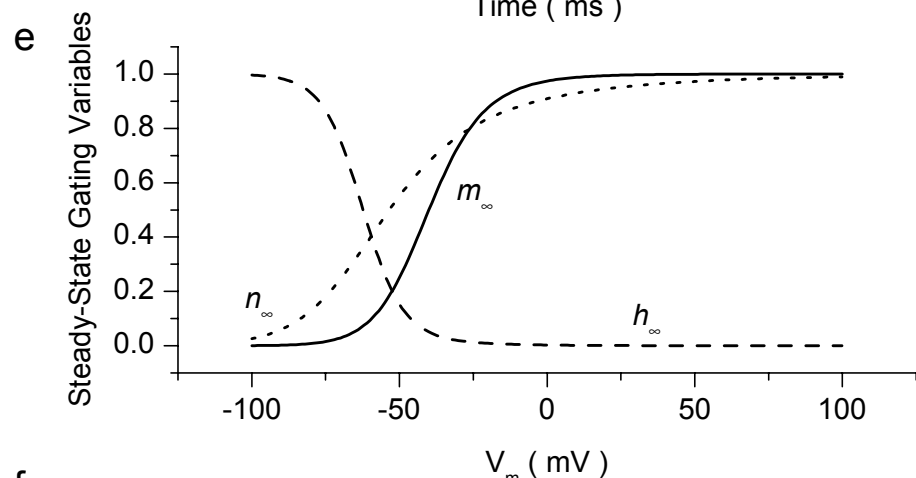
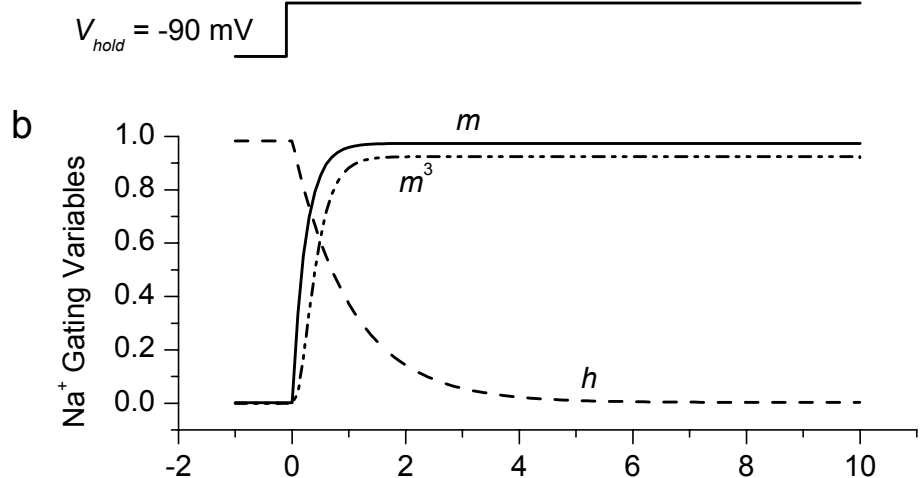
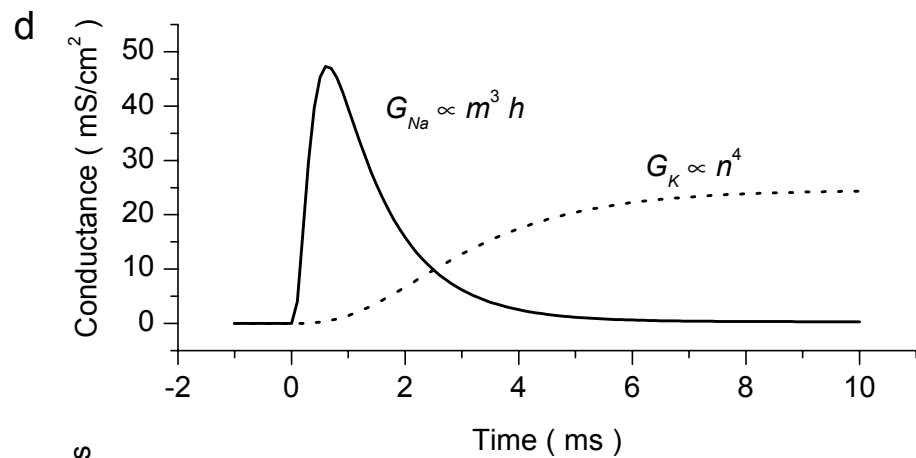
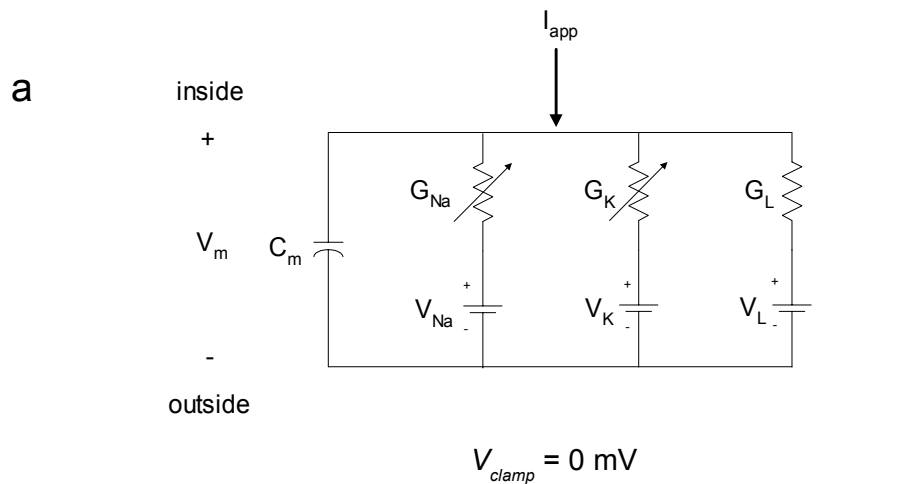
Figure 9. Threshold of the Hodgkin-Huxley model can be explained by examining the stability of “fixed points.” **a-b:** Spiking behavior in the Hodgkin-Huxley model is very sensitive to V_0 , the initial value of voltage. Resting potential (-65 mV) is depicted by the dotted lines). **c:** $\dot{V}(0.5)$, the time derivative of membrane potential at $t = 0.5$ ms, plotted vs. V_0 . Also plotted are the contributions of G_{Na} (dashed line), as well as G_K and G_L (dotted line), to $\dot{V}(0.5)$. This contribution of G_L to the dotted line is minimal, because this conductance is very small. **d:** A magnified plot of $\dot{V}(0.5)$ vs. V_0 . Two fixed points (points where $\dot{V}(0.5) = 0$) are shown. As indicated by the bold arrows, the sign of $\dot{V}(0.5)$ makes the solution flow *toward* the open circle at (-65,0), indicating stability; the solution flows *away* from the open triangle at (-59,0), indicating instability. For $V_0 > -59$ mV, an action potential will be generated.

Table I. Definitions and Units of Mathematical Symbols	
C_m	Membrane capacitance per unit area ($\mu\text{F}/\text{cm}^2$)
$\overline{G}_{Na}, \overline{G}_K$	Maximal values of voltage-gated Na^+ and K^+ conductances per unit area (mS/cm^2)
G_{Na}, G_K	Voltage-gated Na^+ and K^+ conductances per unit area (mS/cm^2)
G_L	Leak conductance per unit area (mS/cm^2)
m, h, n	Voltage-dependent gating variables that determine magnitudes of voltage-gated conductances (dimensionless)
$m_\infty, h_\infty, n_\infty$	Voltage-dependent steady-state values of gating variables (dimensionless)
τ_m, τ_h, τ_n	Voltage-dependent time constants associated with gating variables (ms)
$\frac{dm}{dt}, \frac{dh}{dt}, \frac{dn}{dt}$	Time derivatives of gating variables (1/ms)
V_{Na}, V_K	Equilibrium potentials for Na^+ and K^+ (mV)
V_L	Reversal potential for the multi-ion leak conductance (mV)
I_{app}	Applied current flux ($\mu\text{A}/\text{cm}^2$)
V_m	Membrane potential (mV)
$\frac{dV_m}{dt}, \dot{V}(t)$	Time derivative of membrane potential (mV/ms)

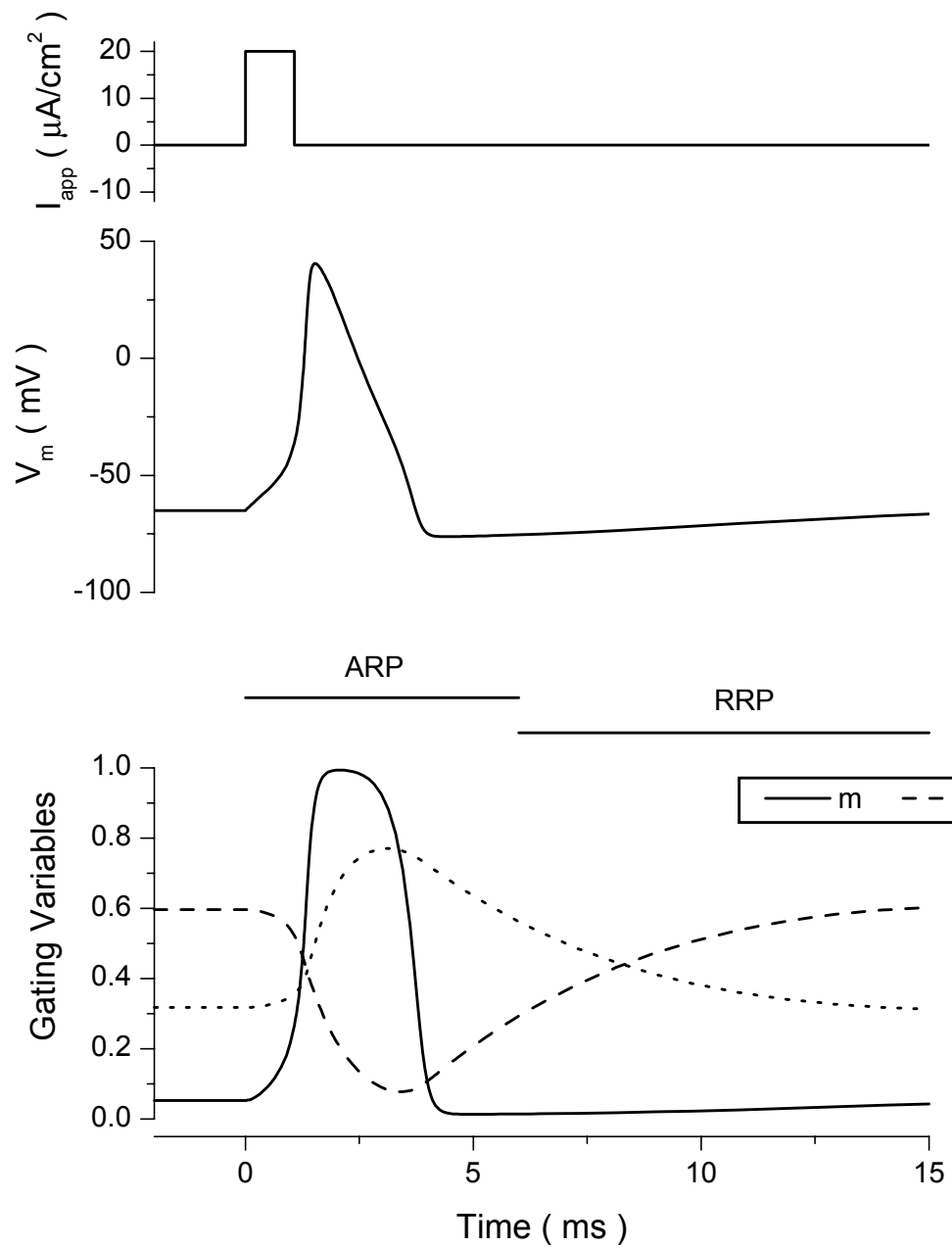




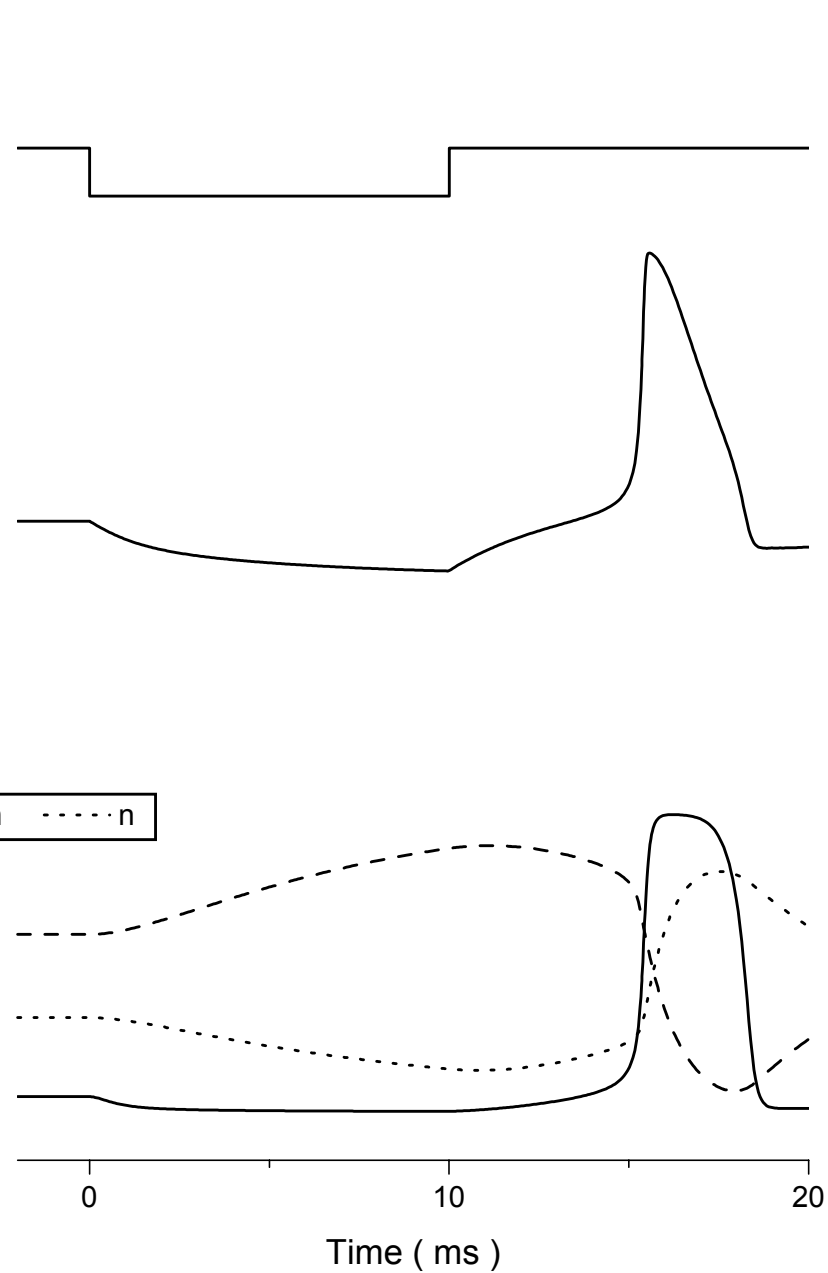




a. Depolarizing Input



b. Hyperpolarizing Input



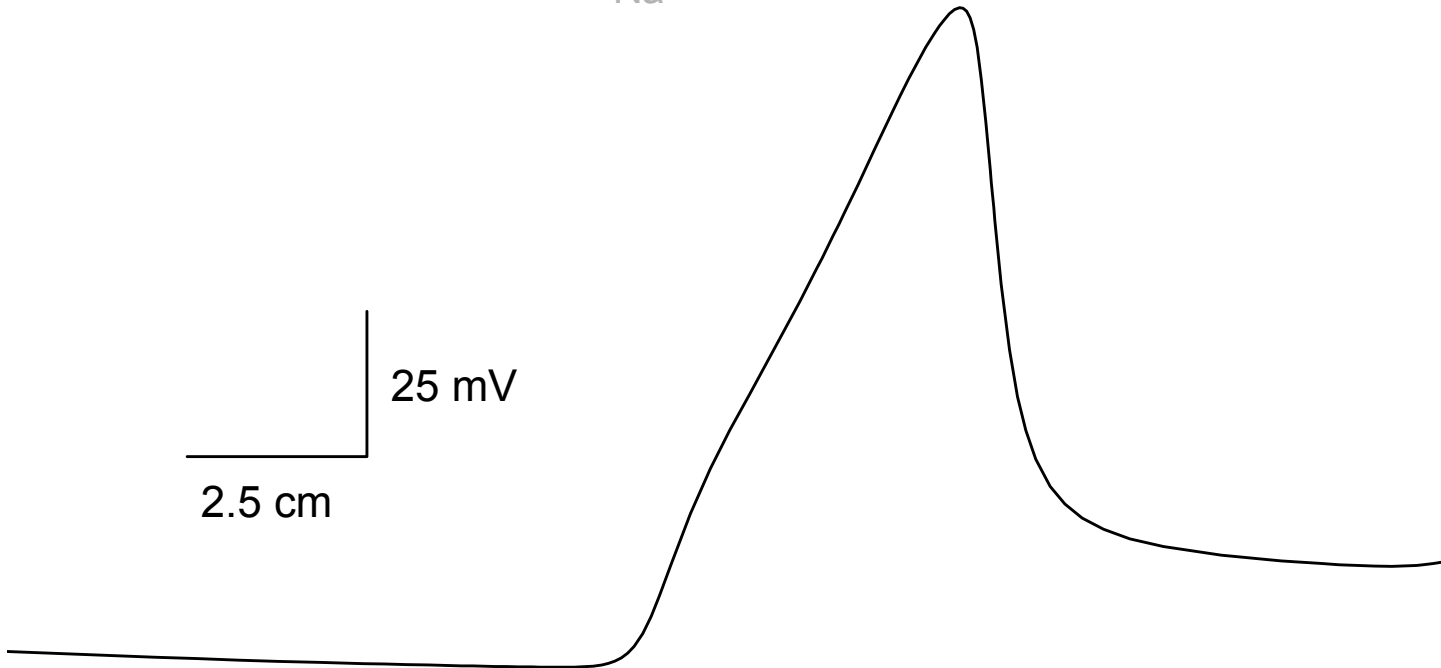
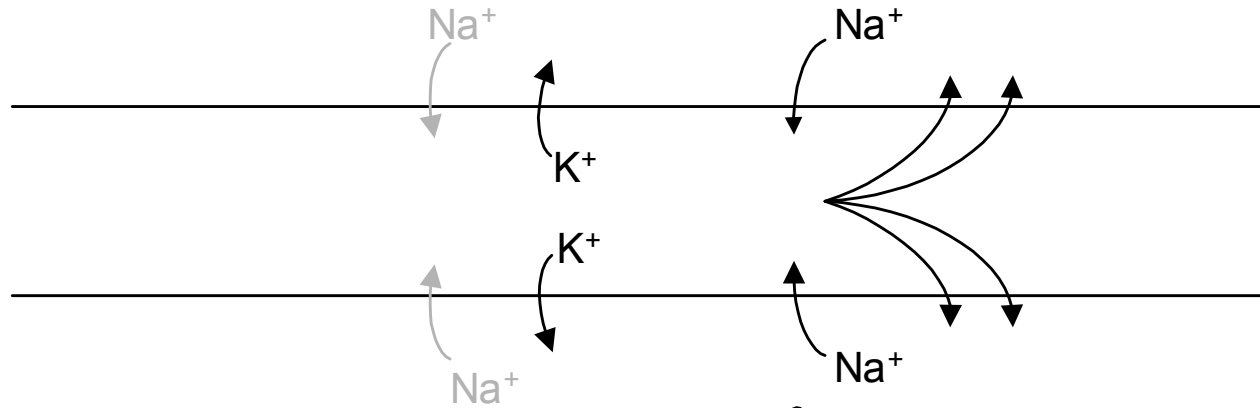
Direction of Propagation

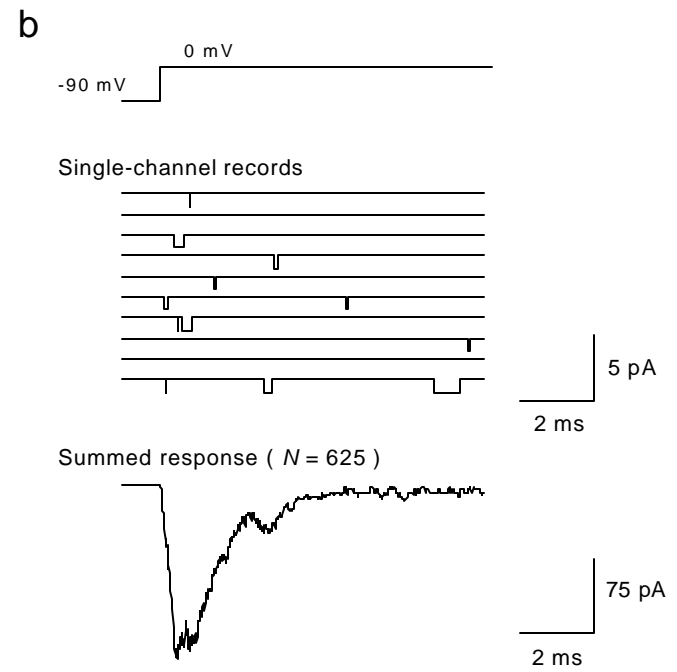
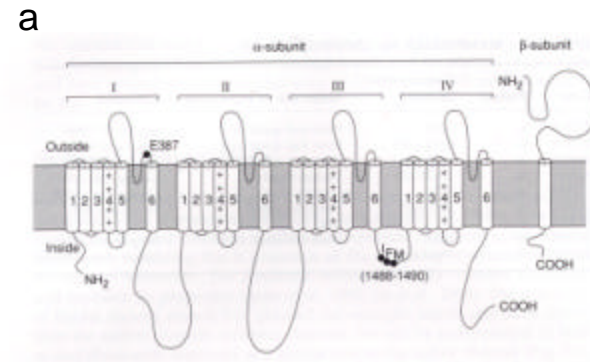


Refractory Membrane

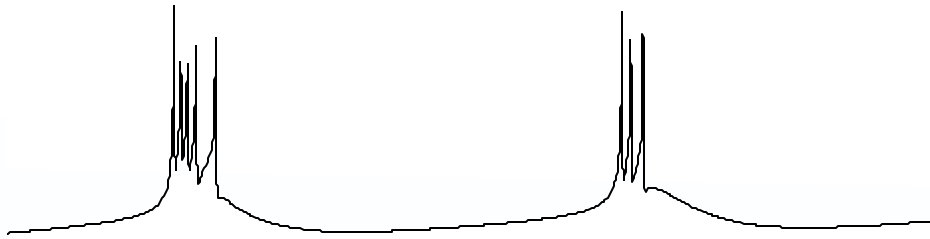
Spiking Membrane

Charging Membrane

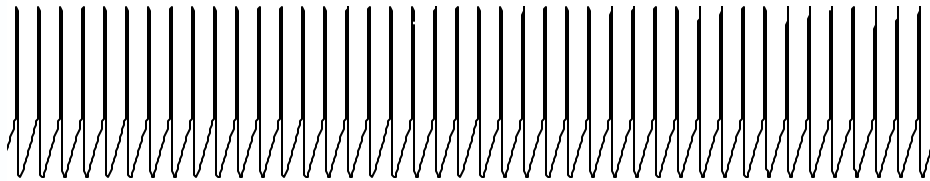




a. Hyperpolarized: Rhythmic Bursting

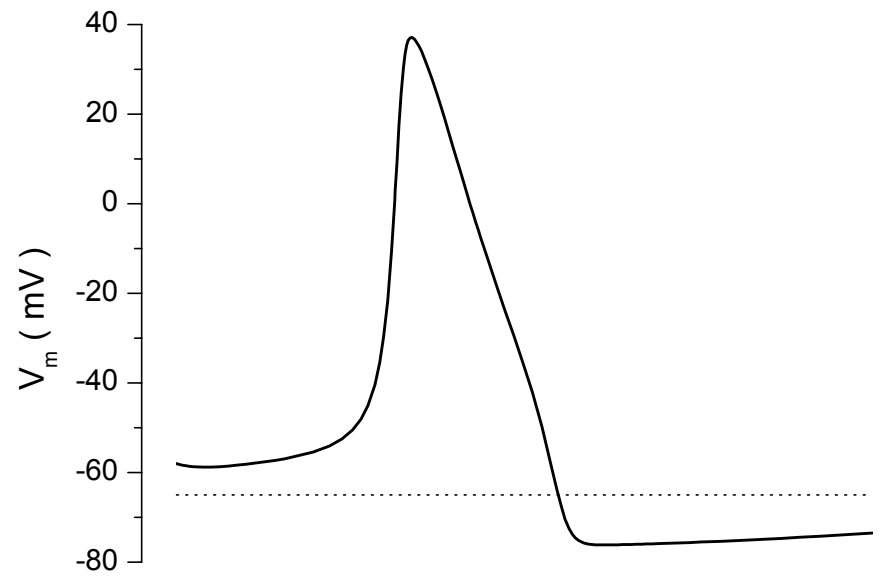


b. Depolarized: Tonic Firing

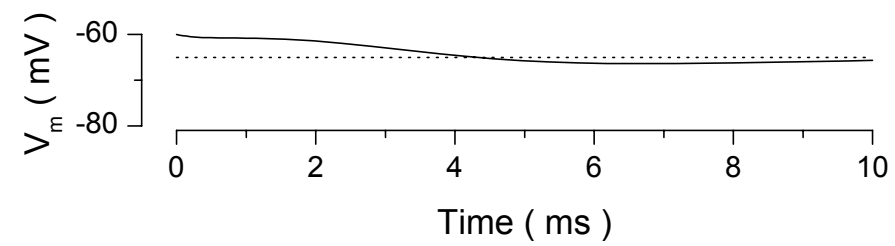


30 mV
100 ms

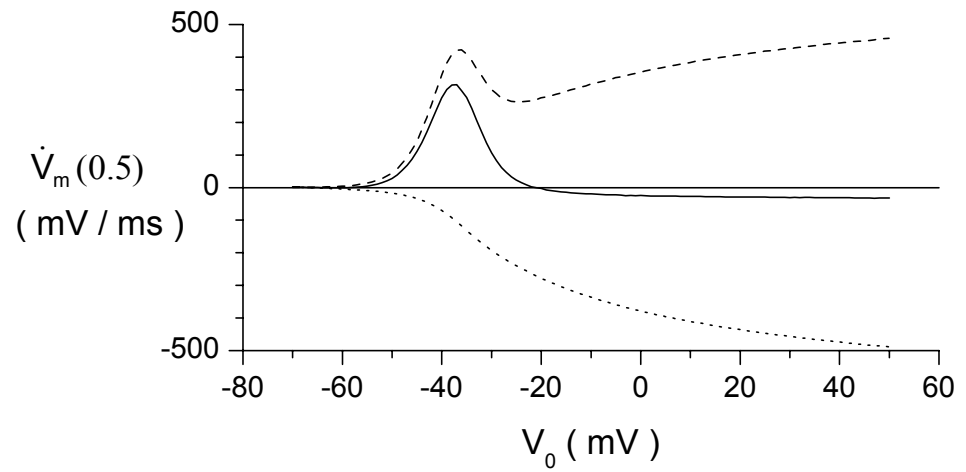
a. $V_0 = -58$ mV



b. $V_0 = -60$ mV



c



d

